Numerical modeling of hydrogen deflagration dynamics in enclosed space*

Yurii Skob[1,*,†], Oksana Pichugina[1,†], Oleksii Kartashov[1,†], Volodymyr Khalturin[1,†], Liudmyla Koliechkina[2,†] and Elena Arshava[3,†]

[1]National Aerospace University "Kharkiv Aviation Institute", 17 Vadym Manko St, Kharkiv, 61070, Ukraine
[2]University of Lodz, 68 Gabriela Narutowicza Str., Lodz, 90-136, Poland
[3]V.N. Karazin Kharkiv National University, 4 Svobody sq., Kharkiv, 61101, Ukraine

Abstract

A three-dimensional mathematical model of gaseous hydrogen combustion in a confined space has been developed. The process is described by a system of differential equations of gas dynamics. The thermodynamic parameters of the mixture and its components are determined as functions of the local temperature and composition of the mixture. Changes in the concentration of fuel and combustion products are determined using conservation laws. The calculation takes into account the rates of decay and formation of components, as well as turbulent diffusion. It is assumed that the chemical reaction occurs only in the volume where the fuel concentration is within the flammability limits. The mathematical model has been tested in comparative tests to predict the combustion of a large-scale hydrogen-air mixture in the open atmosphere. A numerical solution algorithm based on the Godunov method has been developed. A software tool has been developed for the engineering analysis of gas-dynamic processes of hydrogen-air mixture formation and combustion in a closed space with natural ventilation. It enables the prediction of excess pressure, temperature, hydrogen and combustion product concentrations, and other thermo-gas-dynamic parameters of the mixture. This prediction can be used to assess hazardous areas of destruction and recommend safety measures.

Keywords

Fuel-air mixture, Deflagration combustion mode, Fuel mass concentration, Combustion products, Overpressure history, Maximum overpressure, Compression phase impulse

1. Introduction

Assessing the fire safety level of industrial premises is an extremely important task with significant practical significance [1, 2, 3, 4]. A comprehensive investigation of combustion dynamics through mathematical and computational modeling (computational fluid dynamics methods) represents one of the most promising directions of research in this field [5, 6, 7, 8].

A three-dimensional mathematical model of gaseous hydrogen combustion in air within a closed space with natural ventilation is presented, with explicit consideration of combustion product formation.The results of solving some problems obtained using the developed Expert-2 software are provided. First, the results of a comparative experiment on predicting the combustion of a large-scale cloud of hydrogen-air mixture in the open atmosphere, the formation of a spherical shock wave, and the dynamics of temperature and concentration changes are given. Then, a scenario of instantaneous release of highly compressed hydrogen, followed by the formation and combustion of a hydrogen-air mixture in a naturally ventilated industrial facility, is modeled. Calculations were performed to assess the effect of the combustible load on deflagration indicators (total heat release, average excess pressure,

ProfIT AI'25: 5th International Workshop of IT-professionals on Artificial Intelligence, October 15–17, 2025, Liverpool, UK

*You can use this document as the template for preparing your publication. We recommend using the latest version of the ceurart style.

*Corresponding author.
†These authors contributed equally.
y.skob@khai.edu (Y. Skob); o.pichugina@khai.edu (O. Pichugina); o.kartashov@khai.edu (O. Kartashov); v.khalturin@khai.edu (V. Khalturin); lkoliechkina@gmail.com (L. Koliechkina); olena.arshava@karazin.ua (E. Arshava)
0000-0003-3224-1709 (Y. Skob); 0000-0002-7099-8967 (O. Pichugina); 0000-0002-6282-553X (O. Kartashov); 0009-0004-8912-2860 (V. Khalturin); 0000-0002-4079-1201 (L. Koliechkina); 0000-0002-2455-6623 (E. Arshava)

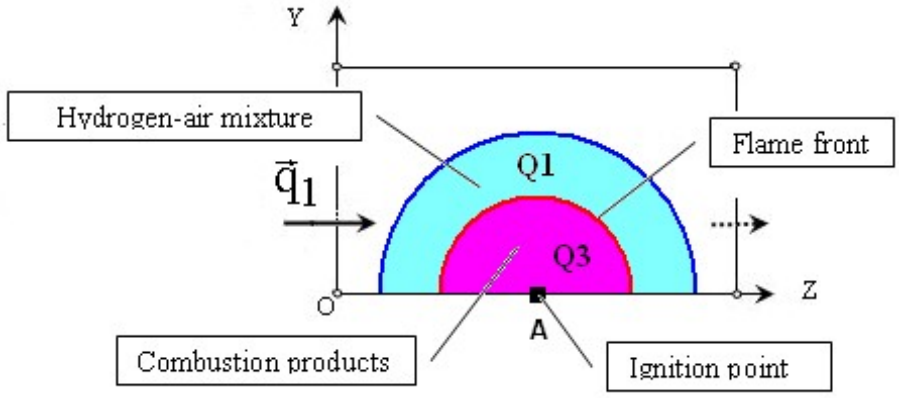

Figure 1: Analytic model of hydrogen-air mixture formation, its combustion, and dispersion of combustion products.

and temperature) in a production facility under various scenarios of deflagration occurrence and development. The peculiarities of hydrogen spread and combustion in air were identified. They are attributed to its low density, high diffusion coefficient, rapid chemical reaction with oxygen, wide ignition concentration limits, and high flame propagation rate.

2. Mathematical model

The most accurate modeling of the physical processes of mixing reactive gases with air [9, 10, 11], their combustion (taking into account the chemical interaction of the mixture components) [11, 12], and the subsequent dispersion of the mixture in open [13, 14, 15] or closed [12, 16, 17] spaces with ventilation is only possible using the system of unsteady Navier-Stokes equations for compressible gas [18, 19, 20]. Effective numerical modeling of turbulent flows is carried out by solving the Reynolds-averaged Navier-Stokes equations, supplemented by a turbulence model [21, 22]. However, most turbulence models do not describe different types of flows with the same degree of adequacy. This is especially true for flows with intense separation and/or large pressure and temperature gradients [23, 24, 25]. Therefore, there is a need to develop innovative mathematical models and computational algorithms for the numerical simulation of such flows.

The main objective of this study is to develop a simplified mathematical model that adequately describes the unsteady processes of mixing reactive gases with air, their combustion, and the subsequent dispersion of the mixture in open or closed spaces with forced or natural ventilation. In addition, the study aims to create an effective numerical solution algorithm and implement it in a computer system that can serve as a tool for modeling these complex gas-dynamic processes.

As a result of the structural analysis of the described flow and the decomposition of the complete gas-dynamic mathematical model, it was assumed that the main influence on the process is exerted by convective exchange of mass, momentum, and energy. Thus, to simulate the mixing processes of a three-component gas, it is sufficient to use the reduced Navier-Stokes equations (Euler approach using source terms). However, the interaction between turbulence and combustion is a powerful feedback mechanism that ensures the exchange of component concentrations, and this phenomenon can be taken into account using source terms in the conservation laws of the mixture components.

The calculation space Ω is a parallelepiped located in the right coordinate system (Figure 1) and divided into spatial cells, the scale of which depends on the characteristic dimensions of the calculation space (roughness of the surfaces being flowed around, dimensions of the objects being flowed around).

The complete system of non-stationary equations describing the three-dimensional flow of a three-component gas mixture is as follows [26, 27, 28, 29, 30, 31, 32, 33, 34, 35] :

$$\frac{\partial \vec{a}}{\partial t} + \frac{\partial \vec{b}}{\partial x} + \frac{\partial \vec{c}}{\partial y} + \frac{\partial \vec{d}}{\partial z} = \rho \vec{f}, \tag{1}$$

where $\vec{a}$, $\vec{b}$, $\vec{c}$, $\vec{d}$, $\vec{f}$ are given by:

$$\vec{a} = [\rho, \rho \cdot u,\ \rho \cdot v,\ \rho \cdot w,\ E]^\top, \tag{2}$$

$$\vec{b} = \left[\rho \cdot u,\ P + \rho \cdot u^2,\ \rho \cdot u \cdot v,\ \rho \cdot u \cdot w,\ (E+P)u\right]^\top, \tag{3}$$

$$\vec{c} = \left[\rho \cdot v,\ \rho \cdot v \cdot u,\ P + \rho \cdot v^2,\ \rho \cdot v \cdot w,\ (E+P)v\right]^\top, \tag{4}$$

$$\vec{d} = \left[\rho \cdot w,\ \rho \cdot w \cdot u,\ \rho \cdot w \cdot v,\ P + \rho w^2,\ (E+P)w\right]^\top, \tag{5}$$

$$\vec{f} = [0, 0, -g, 0, -g \cdot v + e_s/\rho\ ]^\top, \tag{6}$$

where t is time, u, v, w are components of the velocity vector $\vec{q}$, P is pressure, ρ and density,

$$E = \rho(e + \frac{1}{2}(u^2 + v^2 + w^2)) \tag{7}$$

is the total energy per unit volume of the gas mixture, e is internal energy per unit mass of gas; components of vector $\vec{f}$ are projections of distributed volume sources; g is acceleration due to gravity; e_s is heat release intensity per unit volume of gas caused by a chemical reaction.

The conservation laws for the components of the mixture (combustible gas, air, and combustion products), taking into account diffusion and chemical reaction rates, are as follows [36, 37, 38]:

$$\frac{\partial(\rho \cdot Q_i)}{\partial t} + \frac{\partial(\rho \cdot u \cdot Q_i)}{\partial x} + \frac{\partial(\rho \cdot v \cdot Q_i)}{\partial y} + \frac{\partial(\rho \cdot w \cdot Q_i)}{\partial z} = \rho_{Q_{it}} + \rho_{Q_{its}}, \tag{8}$$

where Q_i is the relative mass density of the impurity (the ratio of the density of the gaseous impurity to the density of the mixture); $i = \overline{1,3}$, where $i = 1$ corresponds to fuel, $i = 2$ corresponds to air, $i = 3$ corresponds to combustion products; $\rho_{Q_{it}}$ is the rate of change in impurity density as a result of turbulent diffusion (according to Fick's law, $\rho_{Q_{it}} = div(\rho \cdot \vartheta_D \text{grad} Q_i)$, and the diffusion coefficient ϑ_D is determined according to Berland [39]; $\rho_{Q_{is}}$ is intensity of change in the density of mixture components caused by a chemical reaction.

The system of equations (1)-(8) is incomplete. Therefore, it is supplemented by equations that determine the thermophysical properties of the mixture components.

$$\mu = \frac{1}{\sum\limits_{i=1}^{3} \frac{Q_i}{\mu_i}}; C_P = \sum_{i=1}^{3} Q_i (C_P)_i; C_v = \sum_{i=1}^{3} Q_i (C_v)_i; \sum_{i=1}^{3} Q_i = 1, k = \frac{C_P}{C_v}.$$

For an ideal polytropic gas, the value of e is related to the values of P and ρ of the mixture by the following dependence: $e = \frac{P}{(k-1)\rho}$.

The rate of change in fuel density $\rho_{Q_{is}}$ as a result of a chemical reaction is determined as the product of the molecular mass of the fuel μ_1 and its molar rate of change w_1. It is believed that the chemical "gross" reaction leads to:

$$\sum_{i=1}^{2} \nu_i \chi_i \rightarrow \nu_3 \chi_3,$$

where ν_i is a stoichiometric coefficient, χ_i is a chemical agent ($i = \overline{1,3}$). The molar rate of change w_1 is defined as:

$$w_1 = -\nu_1 A_1 T^{\beta_1} \exp[-E_1/(R\text{T})] \prod_{i=1}^{2} [\chi_i]^{\nu'_i},$$

where R is the universal gas constant, $A_1, \beta_1, E_1, \nu'_1, \nu'_2$ are parameters obtained based on the generalization of experimental data [40, 41, 42], $[\chi_i]$ is the molar concentration of the i-th component of the mixture: $[\chi_i] = \frac{\rho Q_i}{\mu_i \nu_i}$. The Arrhenius reaction constant A_1 was adjusted for use with large control

volumes when solving large-scale problems. The rate of change in the density of combustion products $\rho_{Q_{3s}}$ is determined based on the locomotive mass law:

$$\frac{\rho_{Q_{1s}}}{\mu_1 \cdot \nu_1} = \frac{\rho_{Q_{2s}}}{\mu_2 \cdot \nu_2} = -\frac{\rho_{Q_{3s}}}{\mu_3 \cdot \nu_3}.$$

The heat release intensity e_s per unit volume of gas caused by a chemical reaction is defined as:

$$e_s = -\xi \cdot H_{u1} \cdot \rho_{Q1s},$$

where ξ is the combustion completeness coefficient, H_{u1} is the lower heat of combustion of fuel.

It is assumed that any component of the air flow velocity is subsonic. The oncoming flow is determined by the values of the total enthalpy $I_0^* = \frac{k}{k-1}\frac{P}{\rho} + \frac{1}{2}(u^2 + v^2 + w^2)$, the entropy function $S_0 = \frac{P}{\rho^k}$, the flow velocity vector (angles $\alpha_x,\ \alpha_y,\ \alpha_z$) and relative mass concentration of impurity Q_1 (for gas impurity inflow, $Q_1 \leq 1$). The flow parameters at the inlet are determined using the "left" Riemann invariant relation [43]. On the impermeable surfaces of the calculation cells, the "no leakage" condition is satisfied: $q_n = 0$ (where $\overrightarrow{n}$ is the normal to the cell surface under consideration). The boundary conditions at the outlet of the mixture from the computational domain are specified on the surfaces of the computational cells using the "right" Riemann invariant relation [44].

At the initial moment in time, the parameters of the environment are set in all "gas" cells of the calculation space. In cells occupied by a cloud of impurities, the relative mass concentration of impurities is equal to $Q_1 \leq 1$. In cells with gas evaporation, the law of change in the flow rate of mixture components is set.

3. Numerical algorithm

Vector equation (1) can be represented in integral form for each computational cell:

$$\frac{\partial}{\partial t}\iiint\limits_V a \cdot dV + \oiint\limits_\sigma \hat{A} \cdot d\sigma = \iiint\limits_V \rho \cdot f \cdot dV, \tag{9}$$

where V is the volume of the elementary calculation cell; $\vec{\sigma}$ is the boundary surface of the cell with the external normal $\vec{n}$ $(\vec{\sigma} = \sigma\vec{n})$; $\hat{A}$ is the flux density tensor of conservative variables $\vec{a}$, whose columns are vectors $\vec{b}$, $\vec{c}$, $\vec{d}$, respectively.

The conservation law for each component of the mixture (8) can also be represented in integral form for each computational cell:

$$\frac{\partial}{\partial t}\iiint\limits_V \rho \cdot Q_i \cdot dV + \oiint\limits_\sigma \rho \cdot Q_i \cdot q \cdot d\sigma = \iiint\limits_V (\rho_{Q_{it}} + \rho_{Q_{is}})\, dV. \tag{10}$$

The numerical solution of the fundamental equations of gas dynamics (9), (10) was obtained using the Godunov method [44]. The explicit Godunov method is used to solve Euler's equations, supplemented by the conservation law for the gas mixture concentration in integral form. A first-order finite difference scheme is used to approximate the Euler equations. Second-order central differences are used for the diffusion source term of the gas mixture concentration conservation law. Simple vertical pressure interpolation is applied. The Godunov method has a robust algorithm that is resistant to large-scale disturbances in flow parameters and allows flow parameters to be obtained when modeling the combustion of large-scale gas mixtures. It is assumed that deflagration can occur in the calculation cells where the fuel concentration is within the flammability limits $Q_{1\,\min} \leq Q_1 \leq Q_{1\,\max}$. The values $Q_{1\,\min}$ and $Q_{1\,\max}$ are set based on a generalization of experimental data [45, 46].

Based on the mathematical model, a software has been developed for engineering analysis of gas mixture formation, combustion, and dispersion in the atmosphere. It is used in the Expert-2 research software complex of the Rizikon Risk Research Center (Severodonetsk, Ukraine) and the National Aerospace University "Kharkiv Aviation Institute" (Kharkiv, Ukraine). The software allows various hazardous scenarios to be modeled using standalone computers within a reasonable time frame.

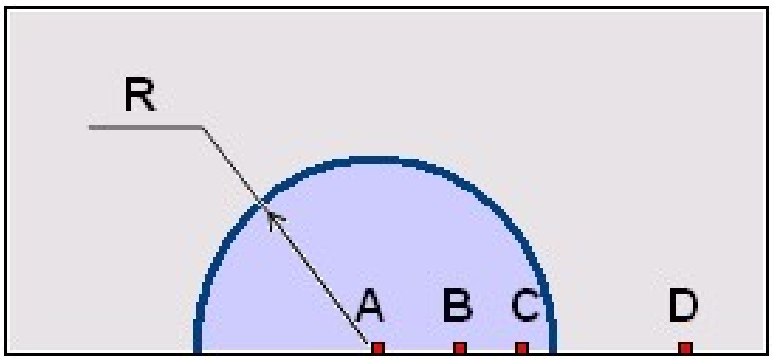

Figure 2: Computation area and control points' location.

4. Mathematical modeling validation

The instantaneous release of combustible gas under high pressure into the atmosphere followed by ignition can generate high-temperature zones and pressure waves. These effects may cause injuries to personnel and damage to vital facilities [47]. Temperature and excess pressure values are typically used to assess pressure and thermal loads on building surfaces [48, 49].

The accepted simplified combustion model is suitable for describing the processes under consideration in both open and closed spaces. Turbulent exchange is taken into account in the laws of conservation of mass of the mixture components (8), (10) in the form of source terms. Experimental data have validated the mathematical model. The deflagration of a hemispherical cloud of a homogeneous stoichiometric hydrogen-air mixture (experiments at the Fraunhofer ICT [50, 51, 52]) is modeled under the following conditions: total cloud volume – 2094m^3; initial pressure – 98.9 kPa; initial temperature – 283 K; radius R of the hemispherical cloud – 10 m. During the calculation, the dynamics of temperature, fuel and combustion product concentration, and pressure are investigated at distances of 5 m (control point B in Figure 2), 8 m (control point C), and 18 m (control point D) from the epicenter of the deflagration (point A).

The calculation space has the following dimensions: length 200 m; width 100 m; height 30 m. The calculation grid has dimensions of $200 \times 100 \times 30$ cells.

Computer specifications: 1 PC with Intel® Celeron® processor (2.4 GHz), 0.75 GB RAM, Windows XP. Processor operating time is 4 hours.

The validation of the mathematical model of hydrogen deflagration against experimental results of measuring excess pressure in the shock wave front was performed by evaluating statistical indicators recommended in the works [53] (Fractional Bias (FB), Geometric Mean Variance (VG), Geometric Mean Bias (MG), Normalized Mean Square Error ($NMSE$), Factor of 2 ($Fa2$), and Correlation Coefficient (r)). Only the initial phase of wavefront compression was studied, as its characteristics are used for the probabilistic assessment of the negative impact of the wave on the environment. For the wave at control point B, the following model performance indicators are obtained: $FB = 0.23, VG = 1.88$, $MG = 1.56, NMSE = 0.29, Fa2 = 71\%$, and $r = 0.78$. At control point C, these indicators have the following values: $FB = -0.18; VG = 2.97;\ MG = 1.07; NMSE = 1.51; Fa2 = 33\%$; $r = 0.01$. For point C, they are as follows: $FB = -0.43; VG = 4.00; MG = 2.39; NMSE = 0.57$; $Fa2 = 42\%; r = 0.63$. The values of the statistical indicators VG, MG, and $Fa2$ for point B, the values of VG, $NMSE$, and $Fa2$ for point C, and the values of VG, MG, $NMSE$, and $Fa2$ for point D slightly exceed the limits recommended in the work [53], which is explained by some desynchronization in the time of passage of the shock wave through the control points compared to the real process.

However, the overall qualitative and quantitative analysis of the compression phase of the shock wave at the control points, taking into account the parameters of the wave's impact on the environment, gives significantly better results: for the maximum excess pressure, we obtained the following indicators' values: $FB = -0.02; VG = 1.04; MG = 0.95; NMSE = 0.04; Fa2 = 100\%; r = 0.72$.

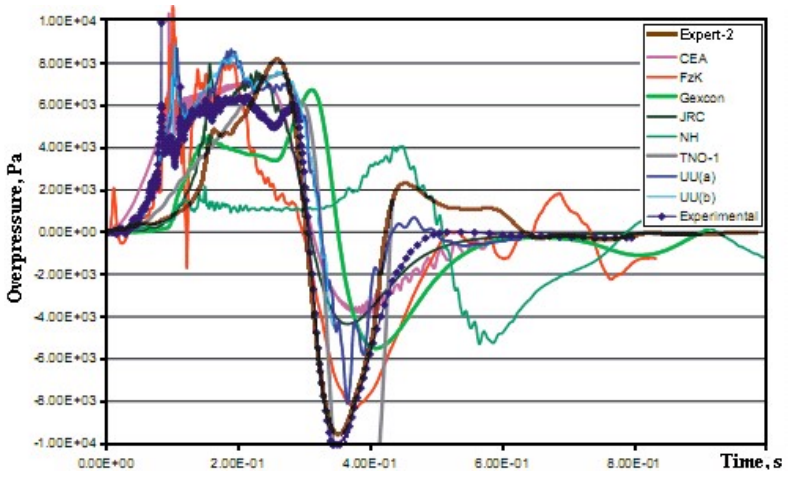

Figure 3: Pressure history in the control point B.

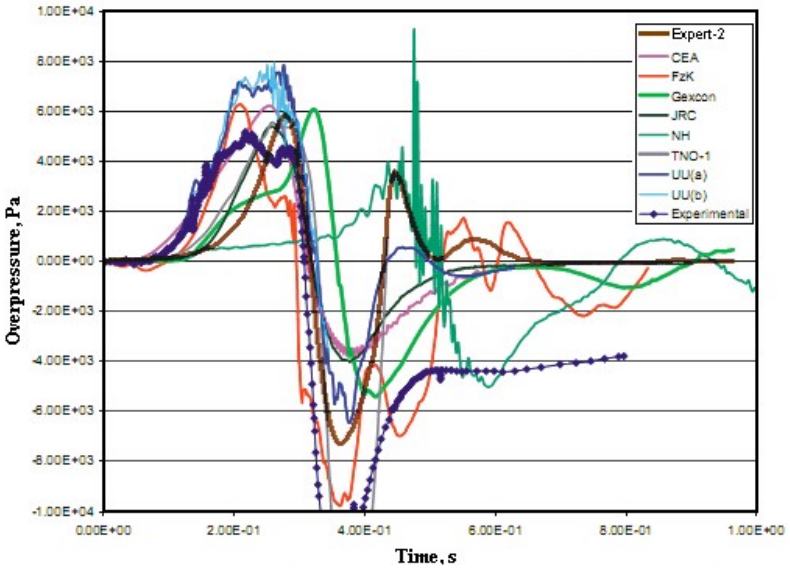

Figure 4: Pressure history in the control point D.

For the compression phase impulse, $FB = 0.14; VG = 1.10; MG = 1.17; NMSE = 0.07;$ $Fa2 = 100\%; r = 0.73$. All relevant model performance indicators are within the recommended limits. Therefore, it can be assumed that the mathematical model of deflagration combustion of a gas-air mixture can be used for the purposes set in the study: to simulate large-scale explosions of a gas-air mixture in the surface layer of the atmosphere; to assess and predict the possible consequences of the baric and thermal effects of combustion products on people and building structures in the epicenter zone of a man-made accident.

The dynamics of excess pressure at control points B and D are shown in Figures 3 and 4 in comparison with experimental data and calculation results obtained using other software [51]. The curves at points B and C are similar. The peculiarities of the combustion model used explain the steeper slope of the calculated curve. The more intense decrease in excess pressure as the shock wave propagates from point C to point D can be attributed to the first-order scheme of the Godunov method.

The temperature dynamics at control points B and D are shown in Figure 5. The flame temperature of the stoichiometric hydrogen-air mixture (Figure 5a) is slightly higher than usual in the experiment, which can be explained by the peculiarities of the model.

In general, the calculation results agree quite well with the experimental data. This allows the developed mathematical model and software to be used to simulate large-scale combustion of a hydrogen-

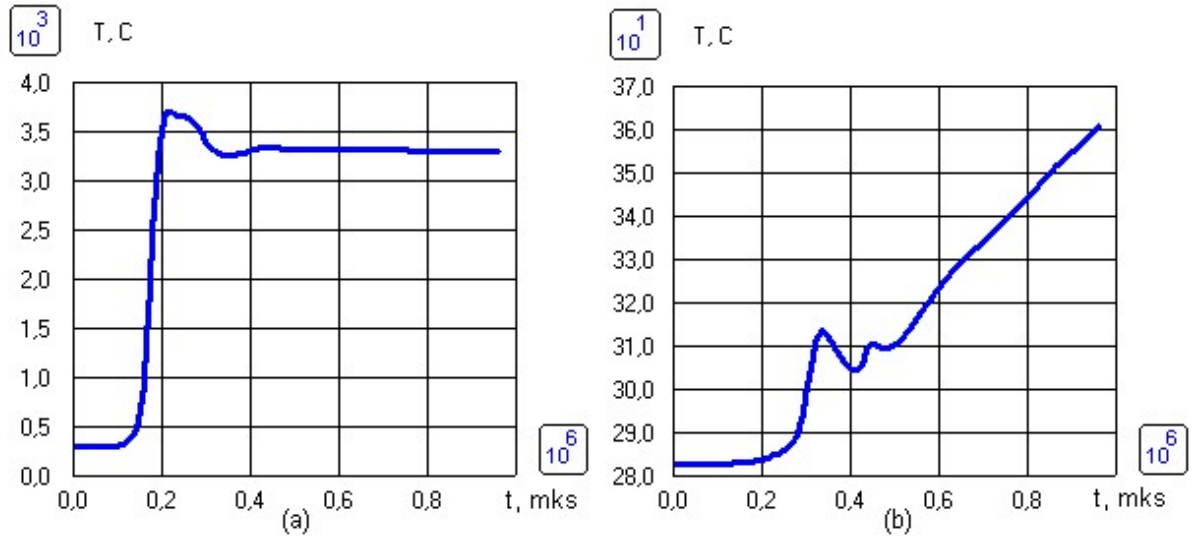

Figure 5: Temperature history in the control points B (a) and D (b).

air mixture in the atmosphere and to predict the barometric and thermal consequences of hydrogen combustion.

5. Hydrogen deflagration modeling in production area

The layout of the enclosed production facility (where hydrogen combustion takes place) is shown in Figure 6. The load-bearing structures of the building are brick walls with a thickness of 0.25 m. The height of the room is 3 m. The room consists of two production subspaces, partially separated by an internal wall 0.25 m thick. The floor thickness is 0.25 m. The room is equipped with two windows (1.5m^2 each) and one doorway (2.5m^2). There are two entrances ($4 \times 2.5\text{m}^2$ each) for hydrogen-powered vehicles. A high-pressure hydrogen cylinder is stored at point A. The production room is located in a three-dimensional space with environmental conditions.

6. Scenarios of deflagration development

Factors such as the location of the deflagration, the position and condition (open or closed) of windows and doorways, and the power and nature of hydrogen release can significantly affect the dynamics of deflagration in a production facility. To determine their impact on the dynamics of deflagration in a production facility, two possible scenarios are modeled with different parameters of the hydrogen cloud (in particular, the mass concentration of hydrogen) (Figure 7).

It is assumed that hydrogen is released as a result of the destruction (or leakage) of a refuelling cylinder stored in the production facility. The production building's doors, windows, and airlocks are open during the deflagration. In the first case, the leak from the cylinder leads to the formation of a stoichiometric hydrogen-air cloud (with a radius of 2 m) with the parameters of the surrounding atmosphere (scenario 1). In the second case, the instantaneous destruction of a refuelling set of 12 cylinders (each with a volume of 0.51m^3) creates a hydrogen-air cloud (with a radius of 2 m) with an ambient temperature, a pressure of 134.213 kPa, and a mass concentration of hydrogen $Q_1 = 0.111$ (scenario 2). It is assumed that for both scenarios, the center of the cloud (and the point of ignition of the flame) is located at point A (Figure 6). The dimensions of the building are $10.5 \times 3.25 \times 12.75\text{m}^3$. The dimensions of the calculation cells are $0.25 \times 0.25 \times 0.25\text{m}^3$. The dimensions of the calculation area are $22.5 \times 4.25 \times 15.75\text{m}^3$. The height of all control points B, C, D, and the deflagration ignition point A (center of the cloud) is 1.125 m.

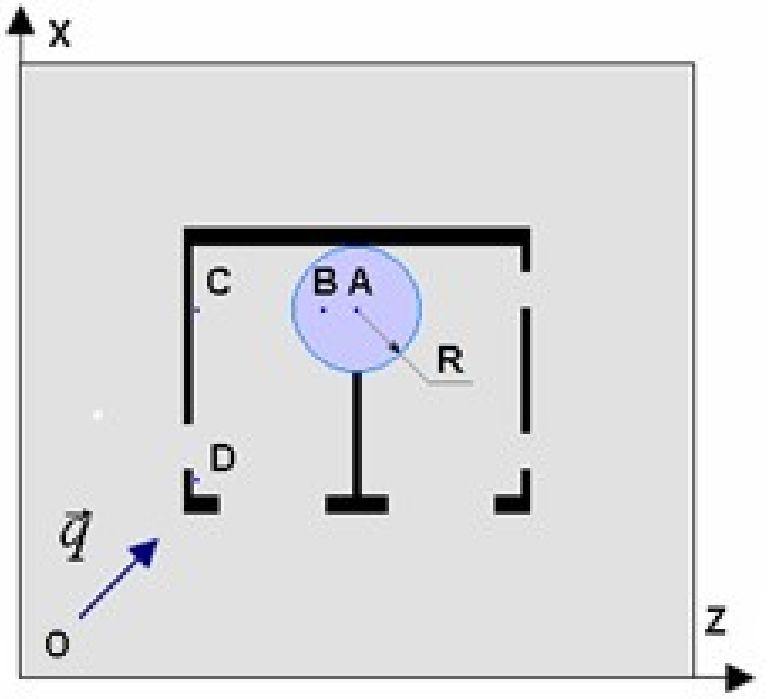

Figure 6: Computation area and control points' location.

7. Deflagration simulation results

To analyze the dynamics of hydrogen deflagration in both scenarios, the following calculated data are considered at control points B, C, and D (Figure 6): dynamics of changes in hydrogen mass concentration over time; dynamics of changes in combustion product mass concentration over time; dynamics of excess pressure and temperature over time.

The distribution of the mass concentration of hydrogen and combustion products in the working area during hydrogen deflagration (0.15, 0.25, and 0.35 s after ignition) for scenario 1 is shown in Figure 7. The pocket of unburned hydrogen (Figure 7b, Figure 7c) can be explained by the influence of the wall. The dynamics of changes in excess pressure and temperature at control point B for scenario 1 are shown in Figure 8. The excess pressure at point C behaves similarly, and the temperature changes are insignificant. The flame temperature of the hydrogen-air mixture (Figure 8b) is again slightly higher than usual in the experiment, which can be explained by the peculiarities of the model. The dynamics of the mass concentration distribution of hydrogen and combustion products in the working zone during hydrogen deflagration (0.10, 0.15, and 0.20 s after the start of deflagration) for scenario 2 is shown in Figure 9. The change in excess pressure and temperature over time at control point B for scenario 2 is shown in Figure 10 (the excess pressure at points C and D behaves similarly to point B, and the temperature changes insignificantly, as in scenario 1).

A comparative analysis of the results of calculations for both scenarios of hydrogen deflagration in a closed zone shows that the control flow parameters differ significantly. In particular, the maximum concentration of combustion products in scenario 2 (Figure 9) is greater than in scenario 1 (Figure 7). The maximum values of excess pressure and temperature in scenario 2 are significantly higher than in scenario 1. These differences are due to the greater mass of hydrogen fuel involved in combustion and the more intense dispersion of the mixture in scenario 2.

The identified features of hydrogen dispersion and combustion in air during deflagration development are due to the low density of hydrogen, high diffusion coefficient, high chemical reaction rate with oxygen, wide range of ignition concentration limits, and high flame propagation rate.

To prevent or minimize the effects of pressure and temperature caused by hydrogen deflagration in a closed production space, some measures are recommended (in the event of high hydrogen concentrations

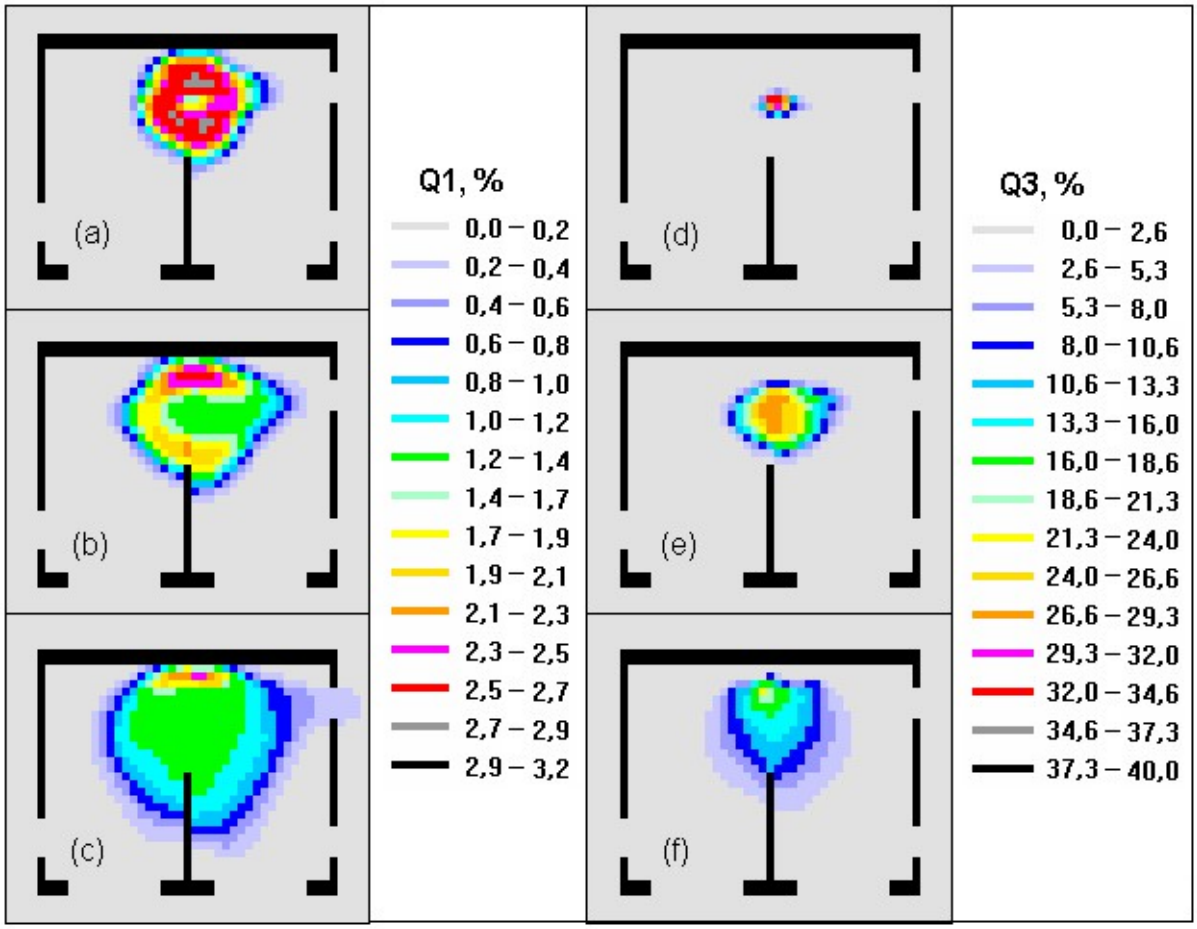

Figure 7: Mass concentration of hydrogen (a-c) and combustion products (d-f) distribution in $0.15, 0.25, 0.35$ s from the moment of inflammation (scenario 1).

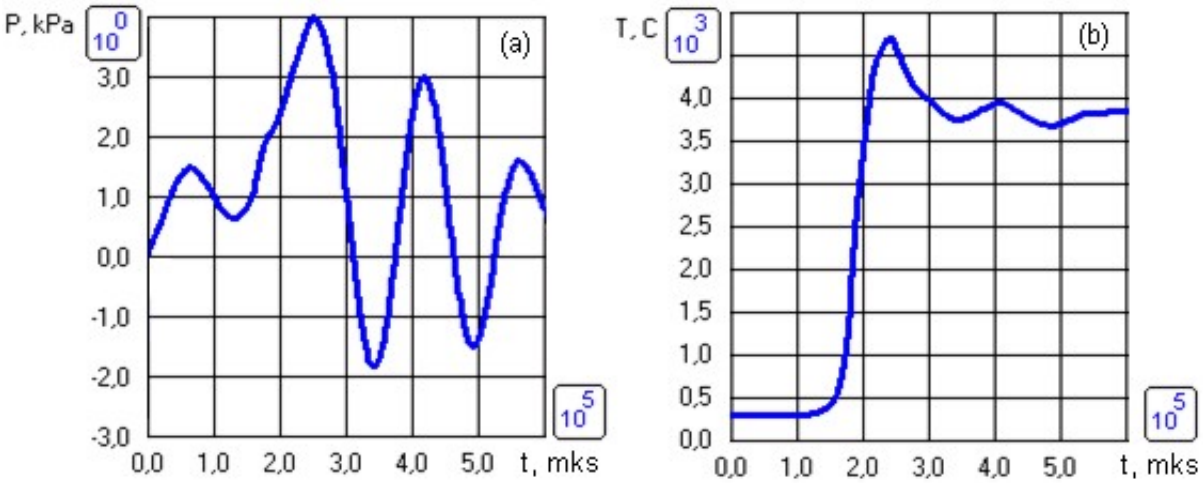

Figure 8: Overpressure (a) and temperature (b) history (point B, scenario 1).

being recorded by sensors): water dispersion (reduces the temperature of the mixture and, as a result, the chemical reaction rate); injection of neutral gas (carbon dioxide) or chemically active additives (increases the minimum ignition concentration limit and, as a result, reduces the temperature of the mixture).

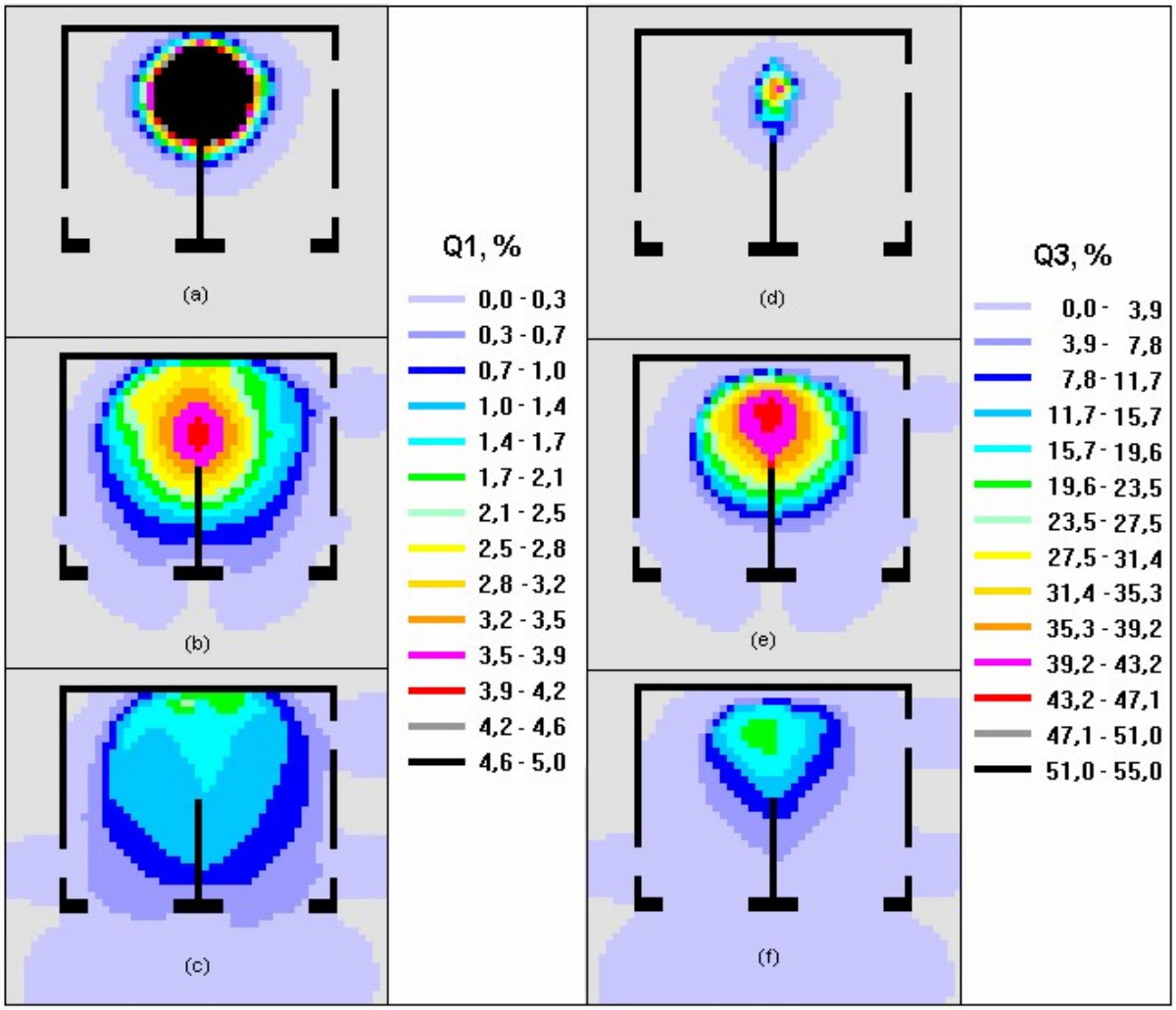

Figure 9: Mass concentration of hydrogen (a-c) and combustion products (d-f) distribution in 0.10, 0.15, 0.20 s from the moment of inflammation (scenario 2).

8. Bridging our model with AI

The results of this study can be used in real-time safety management with the help of artificial intelligence tools, namely reinforcement learning (RL) can be applied to ventilation control. For instance, an RL agent trained on the "digital training ground" of our model can make decisions about opening flaps/extraction speed/water spray, while minimizing $p_{\max}$ and the area of hazardous zones. This directly links RL to the recommendations for reducing concentrations and heat release proposed in the article, thus enabling the improvement of the effect of implementing these recommendations in real-world situations.

9. Conclusion

A three-dimensional mathematical model of gaseous hydrogen combustion in a confined space has been developed. An algorithm for the numerical solution of the system of basic differential equations of gas dynamics based on the Godunov method has been developed. A software has been created for the engineering analysis of gas dynamics processes involved in the formation and combustion of hydrogen-air mixtures in a closed space with natural ventilation, allowing the prediction of changes in excess pressure, temperature, hydrogen and combustion product concentrations, as well as other thermo-gas dynamic parameters of the mixture in the space. This prediction can be used to assess hazardous areas of destruction and recommend safety measures.

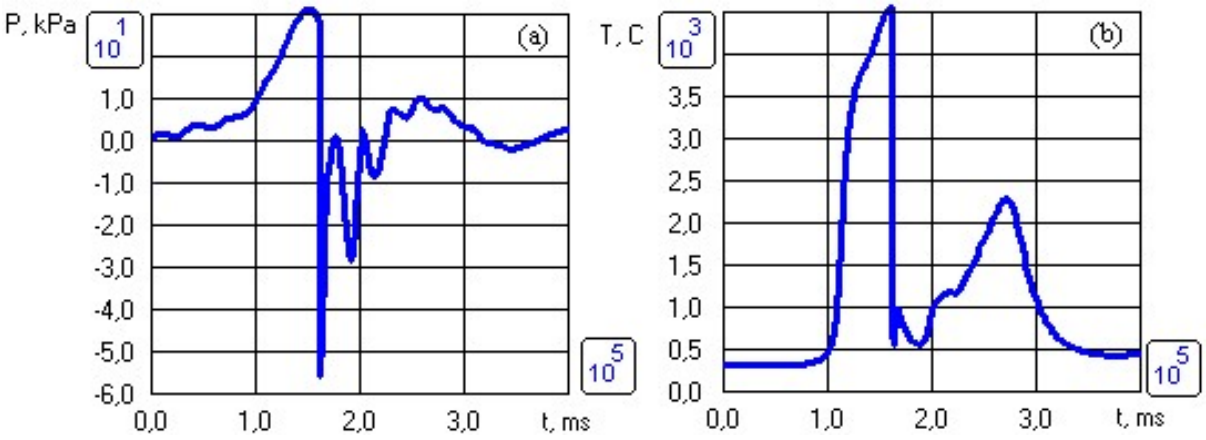

Figure 10: Overpressure (a) and temperature (b) history (point B, scenario 2).

The results of modeling hydrogen deflagration under various initial parameters of a hydrogen-air cloud released in a closed industrial facility are considered. The features of hydrogen propagation and combustion in air during deflagration development are identified due to the low density of hydrogen, high diffusion constant, high chemical reaction rate with oxygen, wide range of ignition concentration limits, and high flame propagation rate. The results of the calculations show that the scale of the deflagration depends on the concentration of hydrogen in the released mixture. Thus, all proposed safety measures that minimize hydrogen concentration can prevent or reduce the barometric and thermal effects caused by hydrogen deflagration in a confined space.

All input decks, meshes, and configuration files used in this study are publicly available at [54].

Declaration on Generative AI

During the preparation of this work, the authors used Grammarly for grammar and spelling checks. Further, the authors used X-GPT-4 for improving the wording of certain paragraphs. After using these tools, the authors reviewed and edited the content as needed and take full responsibility for the publication's content.

References

[1] A. Król, W. Jahn, G. Krajewski, M. Król, W. Węgrzyński, A study on the reliability of modeling of thermocouple response and sprinkler activation during compartment fires, Buildings 12 (2022) 77. doi:10.3390/buildings12010077.

[2] S. Alkış, E. Aksoy, K. Akpınar, Risk assessment of industrial fires for surrounding vulnerable facilities using a multi-criteria decision support approach and GIS, Fire 4 (2021) 53. doi:10.3390/fire4030053.

[3] M. T. Siraj, B. Debnath, S. B. Payel, A. B. M. M. Bari, A. R. M. T. Islam, Analysis of the fire risks and mitigation approaches in the apparel manufacturing industry: Implications toward operational safety and sustainability, Heliyon 9 (2023) e20312. doi:10.1016/j.heliyon.2023.e20312.

[4] W. Ju, G. Su, L. Wu, P. O. Oforiwaa, The 3d-dynamic fire risk evaluation method of modern logistics warehouses: A modified gustav method, Fire Technology 61 (2025) 1199–1232. doi:10.1007/s10694-023-01367-x.

[5] P. W. Agostinelli, D. Laera, I. Chterev, I. Boxx, L. Gicquel, T. Poinsot, Large eddy simulations of mean pressure and h 2 addition effects on the stabilization and dynamics of a partially-premixed swirled-stabilized methane flame, Combustion and Flame 249 (2023) 112592. doi:10.1016/j.combustflame.2022.112592.

[6] M. Kapucu, J. B. W. Kok, CFD-based prediction of combustion dynamics and nonlinear flame transfer functions for a swirl-stabilized high-pressure combustor, Energies 16 (2023) 2515. doi:10.3390/en16062515.

[7] E. Ke, C. Ji, M. Wang, D. Pan, T. Zhu, Prediction of flame transfer function and combustion instability on a partially premixed swirling combustor by the system identification and CFD methods, Aerospace Science and Technology 151 (2024) 109275. doi:10.1016/j.ast.2024.109275.

[8] A. M. Garcia, S. Le Bras, J. Prager, M. Häringer, W. Polifke, Large eddy simulation of the dynamics of lean premixed flames using global reaction mechanisms calibrated for CH4–h2 fuel blends, Physics of Fluids 34 (2022) 095105. doi:10.1063/5.0098898.

[9] V. Y. Basevich, A. A. Belyaev, F. S. Frolov, S. M. Frolov, Turbulent flame propagation in hydrogen-air and methane-air mixtures in the field of synthetic turbulence: Direct numerical simulation, Eng 4 (2023) 748–760. doi:10.3390/eng4010045.

[10] Z. Tai, Q. Chen, X. Niu, Z. Lin, H. Yang, Plasma actuation for the turbulent mixing of fuel droplets and oxidant air in an aerospace combustor, Aerospace 10 (2023) 77. doi:10.3390/aerospace10010077.

[11] W. Cai, J. Wu, Y. Hu, Z. Yang, X. Xue, Y. Lin, Experimental study of fuel-air mixing and dilution jets on outlet temperature distribution in a small gas turbine combustor, Journal of Thermal Science 33 (2024) 1883–1896. doi:10.1007/s11630-024-1983-3.

[12] X. Li, Q. Liu, Y. Ma, G. Wu, Z. Yang, Q. Fu, Simulation study on the combustion and emissions of a diesel engine with different oxygenated blended fuels, Sustainability 16 (2024) 631. doi:10.3390/su16020631.

[13] C. Lejon, D. Vågberg, F. Schönfeldt, B. Liljedahl, L. Persson, J. Burman, D. Elfverson, J. E. Rydman, J. Sjöström, O. Björnham, Lagrangian plume rise and dispersion modelling of the large-scale lithium-ion battery fire in morris, USA, 2021, Air Quality, Atmosphere & Health 17 (2024) 2077–2089. doi:10.1007/s11869-023-01443-9.

[14] L. Gong, S. Yang, Y. Han, K. Jin, L. Lu, Y. Gao, Y. Zhang, Experimental investigation on the dispersion characteristics and concentration distribution of unignited low-temperature hydrogen release, Process Safety and Environmental Protection 160 (2022) 676–682. doi:10.1016/j.psep.2022.02.055.

[15] H. Fossum, E. Åkervik, M. Henriksen, D. Bjerketvedt, Numerical simulation of hydrogen dispersion in an open-ended rectangular channel, International Journal of Hydrogen Energy 92 (2024) 544–559. doi:10.1016/j.ijhydene.2024.10.038.

[16] V. Parsa, A. Santiago, L. Laím, Computational fluid dynamics of compartment fires: A review of methods and applications, Applied Sciences 15 (2025) 2342. doi:10.3390/app15052342.

[17] O. B. Salami, J. F. Brune, G. Xu, A CFD analysis of equipment fires in an underground development heading for improved auxiliary ventilation design, Safety in Extreme Environments 7 (2025) 6. doi:10.1007/s42797-025-00119-0.

[18] H. Elzaabalawy, G. Deng, L. Eça, M. Visonneau, Assessment of solving the RANS equations with two-equation eddy-viscosity models using high-order accurate discretization, Journal of Computational Physics 483 (2023) 112059. doi:10.1016/j.jcp.2023.112059.

[19] M. Hurnik, P. Ciuman, Z. Popiolek, Eddy–viscosity reynolds-averaged navier–stokes modeling of air distribution in a sidewall jet supplied into a room, Energies 17 (2024) 1261. doi:10.3390/en17051261.

[20] E. S. Desyanty, D. E. Kusumaningrum, R. A. Mawarti, A. S. Pahlevi, T. F. Zahra, A. R. R. Nurul, F. Jumaat, S. Purnama, Indonesian cultural education through AR card, in: Proceedings of ELECTRONIC PHYSICS INFORMATICS INTERNATIONAL CONFERENCE (EPIIC) 2023, Tangerang, Indonesia, 2024, p. 040024. doi:10.1063/5.0210208.

[21] W. Sun, Assessment of advanced RANS turbulence models for prediction of complex flows in compressors, Chinese Journal of Aeronautics 36 (2023) 162–177. doi:10.1016/j.cja.2023.06.007.

[22] B. Bhattarai, B. Hilliard, D. Tonina, W. J. Reeder, R. Budwig, B. T. Martin, T. Xing, Evaluation

of reynolds-averaged navier-stokes turbulence models in open channel flow over salmon redds, Journal of Hydrodynamics 36 (2024) 741–756. doi:10.1007/s42241-024-0051-5.

[23] R. Balin, K. E. Jansen, Direct numerical simulation of a turbulent boundary layer with strong pressure gradients 918 (2021) A14. doi:10.1017/jfm.2021.312.

[24] A. Bekhradinasab, J. Al-Zaili, S. Vakilipour, Large eddy simulation of separated flow to investigate heat transfer characteristics in an asymmetric diffuser subjected to constant wall heat flux, International Communications in Heat and Mass Transfer 128 (2021) 105634. doi:10.1016/j.icheatmasstransfer.2021.105634.

[25] N. Xu, I. Bermejo-Moreno, Wall-modeled large-eddy simulations of the flow over a gaussian-shaped bump with a sensor-based blended wall model, Physical Review Fluids 9 (2024) 114605. doi:10.1103/PhysRevFluids.9.114605.

[26] Y. Skob, M. Ugryumov, E. Granovskiy, Numerical assessment of hydrogen explosion consequences in a mine tunnel, International Journal of Hydrogen Energy 46 (2021) 12361–12371. doi:10.1016/j.ijhydene.2020.09.067.

[27] Y. Skob, S. Yakovlev, K. Korobchynskyi, M. Kalinichenko, Numerical assessment of terrain relief influence on consequences for humans exposed to gas explosion overpressure, Computation 11 (2023) 19. doi:10.3390/computation11020019.

[28] Y. Skob, S. Yakovlev, O. Pichugina, M. Kalinichenko, K. Korobchynskyi, A. Hulianytskyi, Numerical evaluation of wind speed influence on accident toxic spill consequences scales, Environmental and Climate Technologies 27 (2023) 450–463. doi:10.2478/rtuect-2023-0033.

[29] Y. Skob, M. Ugryumov, E. Granovskiy, Numerical evaluation of probability of harmful impact caused by toxic spill emergencies, Environmental and Climate Technologies 23 (2019) 1–14. doi:10.2478/rtuect-2019-0075.

[30] Y. Skob, M. Ugryumov, Y. Dreval, Numerical modelling of gas explosion overpressure mitigation effects, Materials Science Forum 1006 (2020) 117–122. doi:10.4028/www.scientific.net/MSF.1006.117.

[31] Y. Skob, M. Ugryumov, Y. Dreval, S. Artemiev, Numerical evaluation of safety wall bending strength during hydrogen explosion, Materials Science Forum 1038 (2021) 430–436. doi:10.4028/www.scientific.net/MSF.1038.430.

[32] Y. Skob, Y. Dreval, A. Vasilchenko, R. Maiboroda, Selection of material and thickness of the protective wall in the conditions of a hydrogen explosion of various power, Key Engineering Materials 952 (2023) 121–129. doi:10.4028/p-ST1VeT.

[33] Y. Skob, S. Yakovlev, O. Pichugina, M. Kalinichenko, Mathematical modelling of gas admixtures release, dispersion and explosion in open atmosphere, in: Proceedings of the 3rd International Workshop of IT-professionals on Artificial Intelligence (ProfIT AI 2023), volume 3641 of *CEUR Workshop Proceedings*, CEUR, Waterloo, Canada, 2023, pp. 168–181. URL: https://ceur-ws.org/Vol-3641/paper15.pdf.

[34] Y. Skob, S. Yakovlev, O. Pichugina, M. Kalinichenko, O. Kartashov, Numerical evaluation of harmful consequences after accidental explosion at a hydrogen filling station, Environmental and Climate Technologies 28 (2024) 181–194. doi:10.2478/rtuect-2024-0015.

[35] Y. Skob, S. Yakovlev, O. Pichugina, O. Kartashov, I. Bychkov, V. Khalturin, Computational estimation of protection wall height impact on hydrogen explosion consequences, Environmental and Climate Technologies 29 (2025) 418–432. doi:10.2478/rtuect-2025-0028.

[36] B. Naud, O. Córdoba, M. Arias-Zugasti, Accurate heat (fourier) and mass (fick and thermodiffusion) multicomponent transport at similar cost as mixture-averaged approximation, Combustion and Flame 249 (2023) 112599. doi:10.1016/j.combustflame.2022.112599.

[37] G. Ferrante, G. Eitelberg, I. Langella, Differential diffusion modelling for LES of premixed and partially premixed flames with presumed FDF, Combustion Theory and Modelling 28 (2024) 695–730. doi:10.1080/13647830.2024.2389099.

[38] A. J. Fillo, J. Schlup, G. Blanquart, K. E. Niemeyer, Assessing the impact of multicomponent diffusion in direct numerical simulations of premixed, high-karlovitz, turbulent flames, Combustion and Flame 223 (2021) 216–229. doi:10.1016/j.combustflame.2020.09.013.

[39] M. E. Berlyand (Ed.), Air Pollution and Atmospheric Diffusion: No. 2, I.P.S.T., New York, 1974.
[40] Y. M. M. Valoy, D. B. Mosiria, J.-C. Sautet, A. Coppalle, Effect of ventilation on carbon monoxide and soot particles emissions in a confined and mechanically-ventilated fire, Fire Safety Journal 138 (2023) 103805. doi:10.1016/j.firesaf.2023.103805.
[41] H. Prétrel, L. Bouaza, S. Suard, Multi-scale analysis of the under-ventilated combustion regime for the case of a fire event in a confined and mechanically ventilated compartment, Fire Safety Journal 120 (2021) 103069. doi:10.1016/j.firesaf.2020.103069.
[42] H. Prétrel, S. Suard, Investigation of the fire mass loss rate in confined and mechanically ventilated enclosures on the basis of a large-scale under-ventilated fire test, Fire Safety Journal 141 (2023) 103962. doi:10.1016/j.firesaf.2023.103962.
[43] P. K. Sweby, Godunov methods, in: E. F. Toro (Ed.), Godunov Methods, Springer US, New York, NY, 2001, pp. 879–898. doi:10.1007/978-1-4615-0663-8_85.
[44] B. Després, Lagrangian godunov schemes, in: G. V. Demidenko, E. Romenski, E. Toro, M. Dumbser (Eds.), Continuum Mechanics, Applied Mathematics and Scientific Computing: Godunov's Legacy, Springer International Publishing, Cham, 2020, pp. 119–124. doi:10.1007/978-3-030-38870-6_16.
[45] A. Z. Mendiburu, J. A. Carvalho, Y. Ju, Flammability limits: A comprehensive review of theory, experiments, and estimation methods, Energy & Fuels 37 (2023) 4151–4197. doi:10.1021/acs.energyfuels.2c03598.
[46] X. Wang, H. Tian, G. Shu, Z. Yang, Study on flammability limit and combustion reactions behaviors of r744/r152a environmentally friendly mixed working fluid by experiments and molecular dynamic simulation, Energy 304 (2024) 131985. doi:10.1016/j.energy.2024.131985.
[47] V. Molkov, D. Cirrone, V. Shentsov, W. Dery, W. Kim, D. Makarov, Dynamics of blast wave and fireball after hydrogen tank rupture in a fire in the open atmosphere, International Journal of Hydrogen Energy 46 (2021) 4644–4665. doi:10.1016/j.ijhydene.2020.10.211.
[48] K. Takeno, H. Kido, H. Takeda, S. Yamamoto, V. Shentsov, D. Makarov, V. Molkov, Flame stabilisation mechanism for under-expanded hydrogen jets, Fire 7 (2024) 48. doi:10.3390/fire7020048.
[49] D. Makarov, V. Shentsov, M. Kuznetsov, V. Molkov, Hydrogen tank rupture in fire in the open atmosphere: Hazard distance defined by fireball, Hydrogen 2 (2021) 134–146. doi:10.3390/hydrogen2010008.
[50] J. García, D. Baraldi, E. Gallego, A. Beccantini, A. Crespo, O. Hansen, S. Høiset, A. Kotchourko, D. Makarov, E. Migoya, An intercomparison exercise on the capabilities of CFD models to reproduce a large-scale hydrogen deflagration in open atmosphere, International Journal of Hydrogen Energy 35 (2010) 4435–4444. doi:10.1016/j.ijhydene.2010.02.011.
[51] E. Gallego, E. Migoya, J. Martinvaldepenas, A. Crespo, J. Garcia, A. Venetsanos, E. Papanikolaou, S. Kumar, E. Studer, Y. Dagba, An intercomparison exercise on the capabilities of CFD models to predict distribution and mixing of h2h2 in a closed vessel, International Journal of Hydrogen Energy 32 (2007) 2235–2245. doi:10.1016/j.ijhydene.2007.04.009.
[52] A. Venetsanos, E. Papanikolaou, M. Delichatsios, J. Garcia, O. Hansen, M. Heitsch, A. Huser, W. Jahn, T. Jordan, J.-M. Lacome, H. Ledin, D. Makarov, P. Middha, E. Studer, A. Tchouvelev, A. Teodorczyk, F. Verbecke, M. Van Der Voort, An inter-comparison exercise on the capabilities of CFD models to predict the short and long term distribution and mixing of hydrogen in a garage, International Journal of Hydrogen Energy 34 (2009) 5912–5923. doi:10.1016/j.ijhydene.2009.01.055.
[53] M. T. Markiewicz, A review of models for the atmospheric dispersion of heavy gases. part II. model quality evaluation, Ecological Chemistry and Engineering S 20 (2013) 763–782. doi:10.2478/eces-2013-0053.
[54] Y. Skob, Input decks, project files, and meshes, 2025. doi:10.6084/M9.FIGSHARE.30281272.